Assessment of benefits obtainable in a Hybrid Solar Vehicle using look-ahead capabilities for incoming solar energy

Gaetano Coraggio, Cecilia Pisanti, Gianfranco Rizzo, Marco Sorrentino
Department of Mechanical Engineering, University of Salerno

Fisciano (SA), 84084, ITALY
E-mail: gcoraggio - cpisanti - grizzo - msorrentino @unisa.it

In order to maximize the benefits of Hybrid Solar Vehicles, battery management should account for two conflicting requirements: at the end of driving the final state of charge (SOC) should be low enough to allow full storage of solar energy captured in the next parking phase, whereas the adoption of an unnecessary constantly-low value of final SOC would give additional energy losses and compromise battery lifetime. The adoption of on-board solar energy prediction can be therefore beneficial to select the best solution in terms of energy management. In order to assess the benefits achievable by using weather forecast, the effects of different strategies of selection of final SOC are studied by simulation over hourly solar data at different months, and the effects of forecast accuracy on fuel economy is analyzed. Finally, the forecast precision achievable by use of available on-line forecast tools is analyzed by comparison with sun power measured data.

Topics: Hybrid Vehicles / Solar Energy / Look Ahead / Energy Management

1. INTRODUCTION

Hybrid Solar Vehicles (HSV), derived by integration of Hybrid Electric Vehicles with Photo-Voltaic sources, may represent a valuable solution to face both energy saving and environmental issues, particularly in urban driving [1,2,8]. Previous studies with optimal design techniques have shown that, in order to maximize the benefits of solar energy, a re-design of the vehicle and powertrain would be necessary [1]. Moreover, the management strategies of a HSV differ significantly from Hybrid Electric Vehicles (HEV), that usually adopt charge sustaining strategies, because the battery can be recharged also during parking time, as it happens for Plug-In Hybrid Electric Vehicles (PHEV). On the other hand, HSV's differ also from these latter vehicles: while for PHEV's the recharge is not free and is mainly finalized to extend the vehicle range, for HSV's the input energy is free, and solar recharge should be maximized not only to extend the range, but mainly to minimize fuel consumption and CO_2 emissions. Therefore, at the end of driving cycle the final state of charge (SOC) should be sufficiently low to make room for the solar energy to be stored in the battery in the next parking phase. But, at the same time, the adoption of an unnecessary low value of final SOC would result in additional battery losses and in reduced fuel economy. The influence of SOC on battery losses also depends on the type of battery, being greater in traditional Lead-Acid batteries and lower with Lithium-Ion batteries. But, apart energy losses, the adoption of very low or high SOC also reduces battery lifecycle, a critical factor for electric and hybrid vehicles.
It therefore emerges the need to estimate the solar energy expected in next parking phase. Moreover, further benefits could be achieved by previous knowledge of driving power [5] and of length of driving cycle, since the most favorable trajectory in attaining the final SOC could be realized.
The recourse to Vehicle to Grid (V2G) technology [6] could partly solve this problem, since the surplus of solar energy could be transferred to the grid, when battery is full. On the other hand, even if this technology will diffuse, it is unlikely that V2G connecting points would be available worldwide in all parking locations, at least in a medium term scenario.
In next chapter, the results of simulation analysis performed on a Hybrid Solar Vehicle for different strategies of selection of final SOC are studied, also considering the effects of solar energy forecast, at different levels of precision. Then, the precision achievable in estimating solar energy by means of on-line weather forecast tools is studied, in order to estimate the benefits that could be achieved in real cases.

2. SOC MANAGEMENT IN A HSV

In the following, the effects of different strategies of selection of final SOC are studied by simulation over hourly solar data at different months and locations, in order to assess the benefits achievable by estimating the energy expected in next parking phase. The simulations are carried out with a dynamic model of a HSV previously developed [1], including a Rule-Based Energy Management Strategy (RBEMS) [5]. This technique considers the effects of operating variables on fuel consumption and SOC, including thermal transient

effects related to engine start and stop, as well as expected daily solar radiation. It has been shown that the fuel consumption obtained by this implementable strategy is very near to the benchmark obtained in off-line by Genetic Algorithms [5].
The RB control architecture consists of two tasks, external and internal, respectively:

1. External task: defines the desired final state of charge to be reached at the end of the driving cycle to enable full storage of solar energy captured during the following parking phase.
2. Internal task: estimates the average power delivered by the ICE-EG (i.e., Internal Combustion Engine – Electric Generator group) and SOC deviation from final state of charge as function of average traction power.

Specifically in this work, the RB strategy was modified so as to incorporate both perfect and real solar prediction to enhance battery management in driving phases. A solar calculator, based on the analysis of time series of solar radiation over about 30 years, has been used [www.nrel.gov/rredc/pvwatts] to estimate the hourly solar energy achievable at different locations and months on a solar roof in horizontal position.

Nominal ICE-EG power [kW]	43
Nominal EM power [kW]	90
Number of Lead-acid battery modules	21
Battery capacity C_B [kWh]	6.3
PV horizontal surface [m^2]	3
Coefficient of drag (Cd)	0.33
Frontal area [m^2]	2.3
Rolling resistance coefficient [/]	0.01
Weight [kg]	1434

Tab. 1. HSV specifications.

	Scenario 1 η_{PV} =0.13		Scenario 2 η_{PV} =0.19		Scenario 3 η_{PV} =0.25	
	Best parametric	Rule 1	Best parametric	Rule 1	Best parametric	Rule 1
[km/l] Jan	20.55	20.55	20.98	21.69	22.29	23.80
[km/l] Jul	26.04	26.59	32.81	33.25	42.50	43.21
Average SOC - Jan	0.62	0.72	0.53	0.73	0.45	0.74
Average SOC - Jul	0.66	0.74	0.61	0.7	0.58	0.69

Tab. 2. Overall resume of the scenario analysis outcomes.

Some results have been recently obtained [7], simulating a Hybrid Solar Vehicle, which characteristics are listed in Tab. 1, over hourly solar data in Los Angeles over ECE-EUDC cycles for three different efficiencies of solar panels. For each case, the best parametric case, obtained with a fixed choice of final SOC, is compared with the result obtained by the rule based approach, using solar energy forecast.

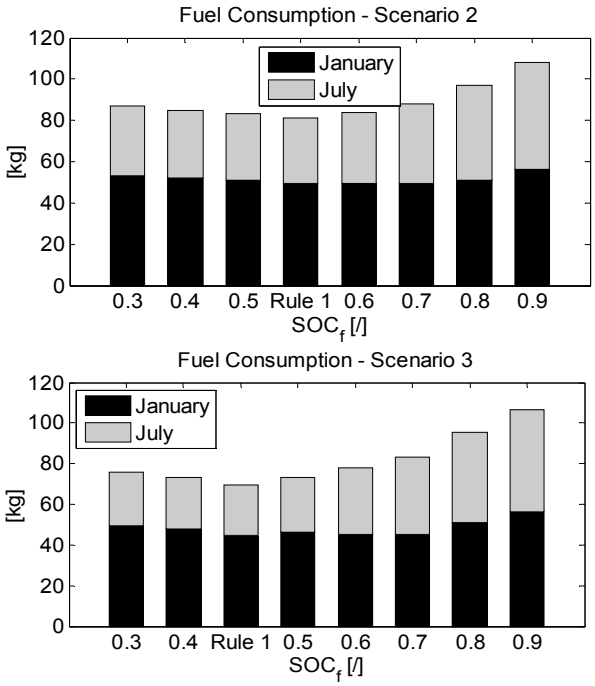

Fig. 1- Simulated Fuel Consumptions for Scenario 2 (ηPV =0.19) and 3 (ηPV =0.25)

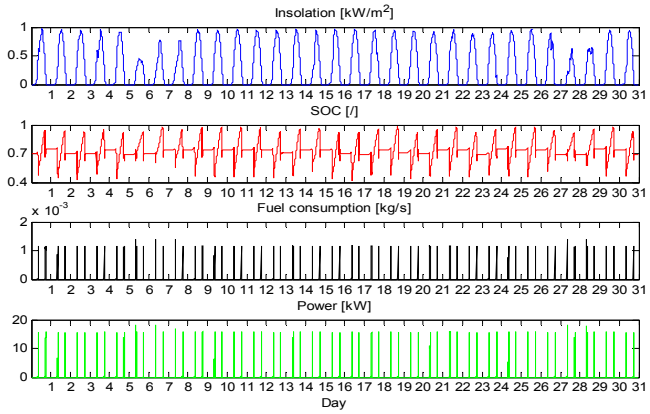

Fig. 2 - Global simulation of July 1988. Scenario 2 optimal case with perfect solar power prediction.

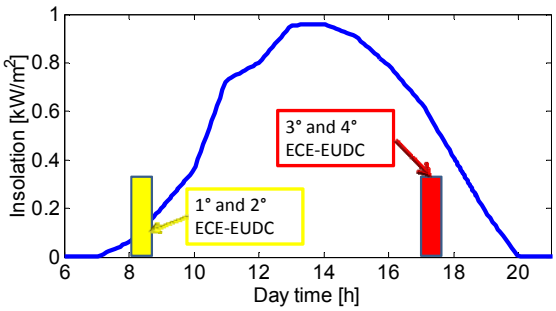

Fig. 3- Schematic representation of a generic daily simulation.

The results confirm that fuel consumption is significantly affected by the choice of final battery SOC, and that the lowest values are obtained by predicting the solar energy available during parking phase (Fig.1). In this case, the occurrences of battery saturation are minimized (fig.2), also avoiding unnecessary operation at low SOC values, where fuel economy is penalized.

2.1.Effects of forecast precision on vehicle management

The results presented in previous figures have been obtained by a perfect prediction of the solar energy that can be captured in next parking phase. This prediction, of course, involves the estimation of both solar power and parking period, in terms of starting/ending time. It is therefore important to evaluate the sensitivity of the fuel consumption reduction to the precision in estimating the incoming solar energy. A series of simulations have been performed, introducing errors with respect to perfect prediction (the estimation of final SOC is performed with the perturbed data, while the simulation of fuel consumption utilizes the original data). The expected solar power data have been modified by introducing a Gaussian error, according the following formula:

$$P = P_{ref} + P_{ref,max} k\, RN \qquad (1)$$

The real power value P_{ref} is perturbed by adding a positive or negative term proportional to the maximum power during the day. RN indicates a random number from a normal distribution with zero mean and standard deviation one. The factor k has been varied between 0 and 0.4.

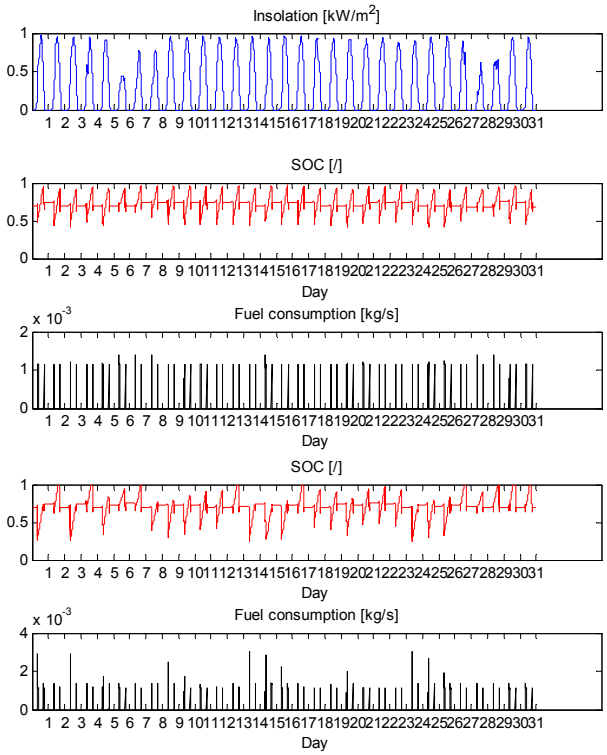

Fig. 4. Comparison between perfect (k=0, up) and non perfect (k=0.4, bottom) prediction.

A comparison between the results obtained by perfect (k=0) and inaccurate (k=0.4) prediction is presented in Fig. **4**. It can be observed that, for perfect prediction, SOC values range usually from 0.5 to 0.9, while in case of inaccurate prediction they range in a wider interval, in some cases reaching saturation conditions (SOC=1). Consequently, fuel consumption values are quite regular in the former case, while some irregular peaks are present in case of inaccurate prediction.

The results obtained by simulation analysis are summarized in next figures, in terms of fuel economy (Fig. 5) and percent degradation (Fig. 6) with respect to perfect prediction. In both cases, the best result obtained by parametric analysis, using a fixed value of final SOC, is also indicated (red line). It can be observed that, as expected, fuel economy decreases when forecast error increases. Moreover, the spread of the results also increases significantly with forecast error. In particular, if forecast error is lower the about 0.15, the results obtained by use of solar power forecast are better than the best result obtained by a fixed value of SOC, while for higher errors there is not an apparent benefit in terms of fuel economy by using weather forecast.

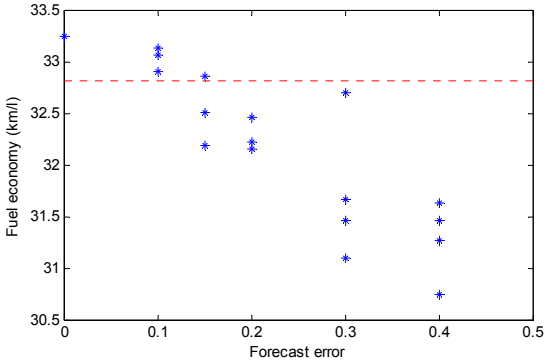

Fig. 5. Fuel economy vs forecast error (red line is the best parametric result).

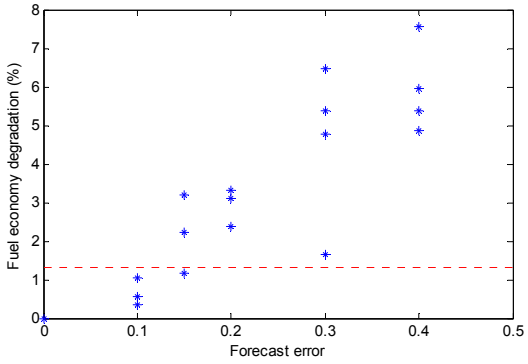

Fig. 6. Fuel economy percent degradation vs forecast error (red line is the best parametric result).

Anyway, it should be observed that the reference case considered (red line) represent the best result obtained by a parametric analysis, optimized for the months in study, and that the fuel economy values obtained by a non optimized fixed value of final SOC would be lower.

3. SOLAR POWER FORECAST

The estimation of net incoming energy in next parking phase involves the estimation of both solar power and of

parking time. The estimation of the start of next parking phase could be accomplished by use of on-board navigator system, providing the expected end of the current driving cycle. Regard to the end of parking phase, this could be estimated starting from statistical data on the driver habits, also considering the influence of the day of the week. Alternatively, the driver could be asked to enter or confirm these data when starting a new driving cycle.

In the following, the accuracy achievable in solar power forecast by using some on-line tools is analyzed. There are many websites that offer weather forecast, for different locations. Moreover, there are an increasing number of companies that offer forecasting for the energy sector, including solar power prediction, as for instance www.enfor.eu, claimed as "among the most accurate tools on the market for solar power forecasting today". Anyway, this tool is not currently available on-line. For this study, it has been selected www.wunderground.com, a service available on-line that allow to obtain forecasts for 5 days for a generic location. The site does not show the expected solar power, but instead provides the expected cloud cover, in percent, at various hours of the day (1, 4, 7, 10, 13, 17, 19, 23). This index can be correlated to solar power, according to some studies [4]. The forecast is based on interpolation from weather stations near to the given location.

A software tool to extract cloud cover estimation for a given location has been developed and implemented in Matlab on a web server. In fig.4 an example of cloud cover forecast is shown, for the current day and for the three subsequent days.

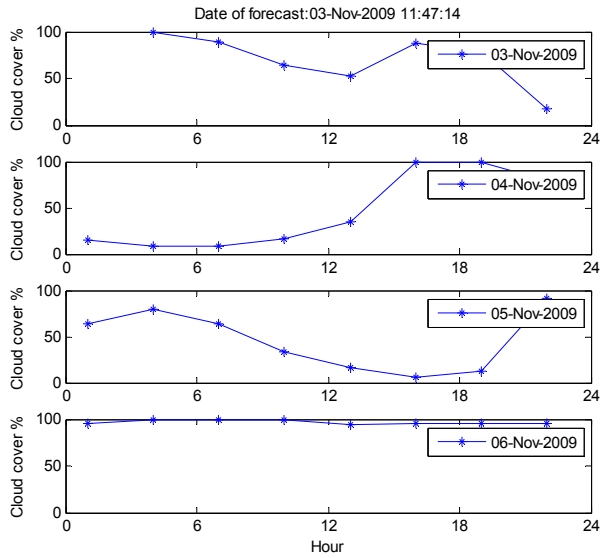

Fig. 7 - Cloud cover forecast for Fisciano, Italy

In order to check the possibility to use such data for estimation, the global solar radiation on an horizontal plane in Fisciano has been measured by means of a pyranometer, in a period from March 21 to May 9, 2010. The data have been aggregated as hourly average. In parallel, cloud cover forecast data have been acquired on-line. For each day, the measured data E_m have been compared with theoretical radiation E_s, computed considering direct and diffused components in a sunny day, and the ratio f between them has been computed:

$$f = \frac{E_m}{E_s} \tag{1}$$

The formulas to calculate solar radiation, in absence of clouds, can be found in several references [9, 10]. In the following, the relationships used in this paper are presented. The variables defining sun position (declination δ, hour angle h, height ϑ_s, azimuth Φs) are computed by the following relationships, as a function of Latitude L and longitude φ:

$$\delta = -23.45 \cdot \cos\left(\frac{2\pi(N+10)}{365}\right) \tag{2}$$

$$h = -180 + 360\frac{hour}{24} \tag{3}$$

$$\vartheta_s = arcsin(cos(h)\cos(\delta)\cos(\varphi) + \sin(\delta)\sin(\varphi)) \tag{4}$$

$$\Phi_s = \sin^{-1}\frac{\cos\delta \sin h}{\cos\vartheta_s} \tag{5}$$

where *hour* indicates local time, computed also considering local longitude. The mean instantaneous direct radiation on horizontal surface is about I_0=1356$\frac{W}{m^2}$. Considering that p_0 is the pressure at sea level, p_z is the pressure of the place considered, it is possible to calculate the air mass at sea level (m_0) and the air mass in the place considered (m_z).

$$m_0 = \frac{1}{\sin(\vartheta_s)} \tag{6}$$

$$m_z = m_0\frac{p_z}{p_0} \tag{7}$$

The transmittance of direct radiation is τ_b:

$$\tau_b = e^{-\frac{0.65m_z}{2}-\frac{0.095m_z}{2}} \tag{8}$$

$$I_{bn=}I_0 \cdot \tau_b \tag{9}$$

The direct solar radiation can be computed as a function of the angle of incidence *i*:

$$E_b = I_{bn}\cos(i) \tag{10}$$

To compute the solar radiation diffuse it is necessary to know the factor angle of diffuse radiation (R_d), the mean instantaneous direct radiation on horizontal surface (I_{d0}) and the orientation of the horizontal surface respect the south (ϕ_v).

$$R_d = \cos(\phi_v)^2 \tag{11}$$

$$\tau_d = 0.2710 - 0.2939\tau_b \tag{12}$$

$$I_{d0} = I_0\sin(\vartheta_s) \tag{13}$$

So the diffuse radiation is:

$$E_d = I_{d0}R_d \tag{14}$$

Finally the global solar radiation can be computed:

$$E_s = E_b + E_d \tag{15}$$

Next pictures show a comparison between measured and computed values, and the cloud cover data for the

same day (this value has been acquired at the end of the day). In the first case, with an average cloud cover of 12% (Fig. 8), the daily measured radiation is about 94% of the theoretical one, while in the second case (Fig. 9) the measured radiation is significantly lower (about 50%), consistently with a higher value of cloud cover (34.5 %).

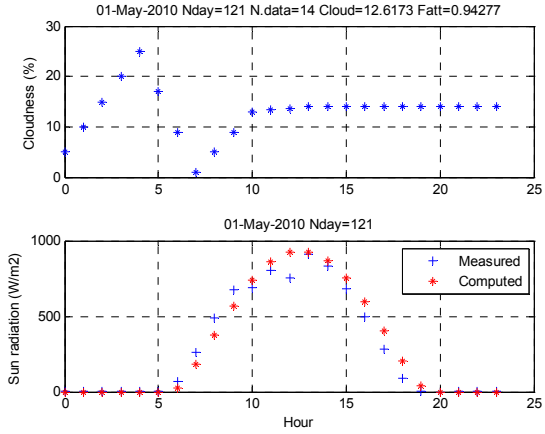

Fig. 8. Measured and computed solar radiation, and estimated cloud cover (May 1st, 2010).

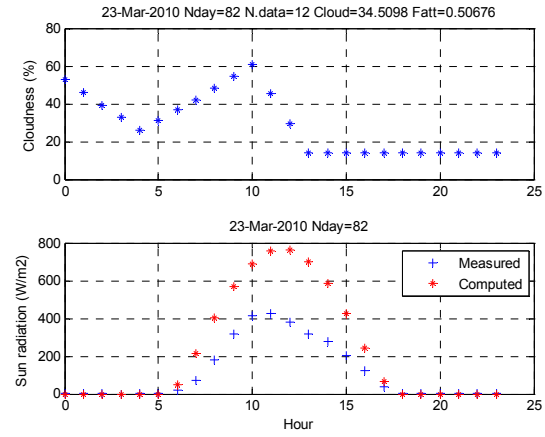

Fig. 9. Measured and computed solar radiation, and estimated cloud cover (March 23rd, 2010)

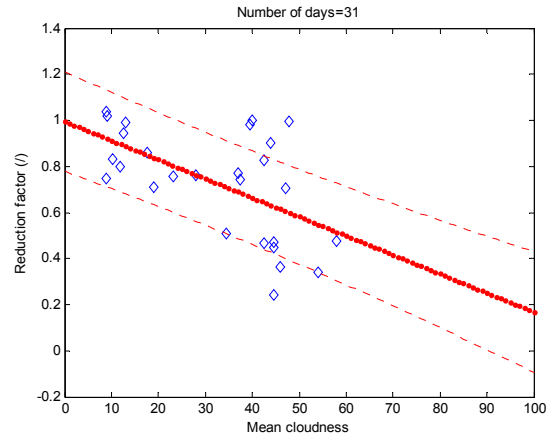

Fig. 10. Reduction in daily solar energy vs cloud cover

Anyway, the study of the whole data has shown that there is not a significant correlation between the hourly cloud cover and the difference between measured and theoretical data, with a correlation coefficient almost equal to zero. This poor correlation may depend on several factors, as the need to interpolate from different and possibly distant weather stations.

Instead, better results can be found by aggregating the data on a daily base. In Fig. 10, the ratio f (1) is plotted versus the daily mean cloud cover, while the red line represents the first-order regression curve. In Fig. 11, the error between the measured value of f and the value estimated by the regression line is plotted, versus mean daily cloud cover.

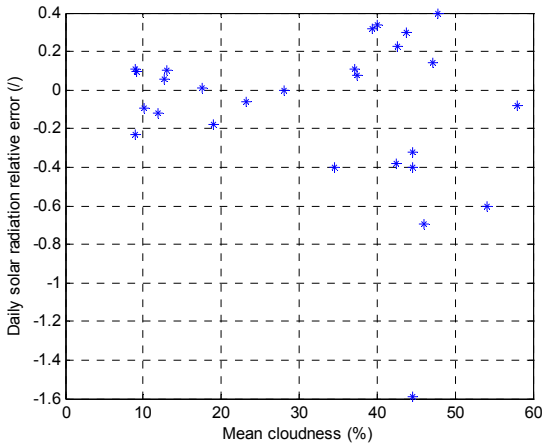

Fig. 11. Distribution of forecast error on daily base

By analyzing the data corresponding to 31 days, and considering only days with at least 10 hourly measured data per day, it emerges that, when could cover is less than 30%, the relative error between the measured value and the value estimated by regression line is lower that 20%, while with higher values of cloud cover (30-60%) the uncertainty is larger, usually within 40%, apart some singular cases. It can be observed that with cloud cover between 40% and 50% there are roughly two clusters of data: one under the red line, corresponding to days with a reduced radiation, and one up the red line, corresponding to days with little reduction in radiation with respect to sunny day. At higher cloud cover (50-60%) the trend appears more regular. It could be considered that, when cloud cover is limited, the probability that clouds could obstruct sun rays is lower, and the data are more scattered, while the randomness is lower at low and high cloud cover values.

Anyway, these conclusions should be confirmed by the analysis of a longer series of data, spanning over different periods of the year and, of course, extended to different locations.

However, it should be remarked that the factor k used in equation (1) does not coincide with the relative error plotted in Fig. 11, although they are of course correlated.

4. CONCLUSIONS

In order to maximize the benefits obtainable with Hybrid Solar Vehicles, more advanced look ahead capabilities would be required. In particular, the optimum compromise between two potentially

conflicting aspects should be realized: i) to leave as much as possible room in the battery for solar recharge and ii) operate in a favorable battery SOC range in terms of energy losses and life cycle. The future recourse to V2G technology would reduce but not remove the need to estimate the net incoming energy. Simulation results at different months and locations have shown that the estimation of the incoming solar energy in next parking phase produces a more efficient energy management, with reduction in fuel consumption, particularly at higher solar radiation. It has also been analyzed how these benefits deteriorate in presence of forecast inaccuracy.

It has also been studied how measured solar power is correlated to cloud cover, using an a software tool available on-line. The results show that there is a significant scatter between the measured data and the data estimated by a regression line as a function of mean cloud cover, particularly when this index ranges from 30 and 50%. Anyway, the simulations performed have shown that the adoption of solar energy prediction can give interesting benefits on fuel economy even in presence of forecast errors within 10-15%.

Future developments include the study of other specialized tools for solar power prediction recently available on the market, in order to assess their accuracy. Moreover, the study, performed on a Lead-Acid battery, should be extended to other type of batteries, as Lithium Ion, also considering more articulate scenario's, including random variations in driving cycle profile, length and parking time.

5. REFERENCES

[1] Arsie, I., Rizzo, G., Sorrentino, M. (2007) "Optimal Design and Dynamic Simulation of a Hybrid Solar Vehicle", SAE Transactions - Journal of Engines, Vol. 115-3, pp. 805-811.

[2] Arsie, I., Rizzo, G., Sorrentino, M. (2008), "A Model for the Optimal Design of a Hybrid Solar Vehicle", Review of Automotive Engineering, Vol. 29:3, pp. 439-447.

[3] Marano V., Tulpule P., Stockar S., Onori S., Rizzoni G., Comparative study of different control strategies for Plug-In Hybrid Electric Vehicles (2009). SAE Paper 2009-24-0071, 9th International Conference on Engines and Vehicles (ICE 2009), Sep 13-18, 2009, Capri (Italy).

[4] Nielsen, L., Prahm, L., Berkowicz, R., Conradsen, K., (1981), "Net incoming radiation estimated from hourly global radiation and/or cloud observations". J. Climatol. 1, 255–272.

[5] Sorrentino, M., Rizzo, G., Arsie, I., (2009) "Analysis of Rule-Based Control Strategies for On-Board Energy Management of Hybrid Solar Vehicles", Proc. of E-COSM'09, the 2009 IFAC Workshop on Engine and Powertrain Control, Simulation and Modeling. Rueil-Malmaison, France, November 30-December 2, 2009.

[6] Kemption W., Tomic J., Letendre S., Brooks A., Lipman T, - Vehicle to Grid Power: Battery, Hybrid, and Fuel Cell Vehiccles as Resources for Distriubted Electric Power in California, UCD-ITS-RR-01-03, 2001 http://www.udel.edu/V2G/docs/V2G-Cal-2001.pdf

[7] Rizzo G., Sorrentino M. (2010), "Introducing Sunshine Forecast to Improve On-Board Energy Management of Hybrid Solar Vehicles", IFAC Symposium Advances in Automotive Control, July 12 - 14 2010, Munich, Germany.

[8] Rizzo G., (2010), "Automotive Applications of Solar Energy", IFAC Symposium Advances in Automotive Control, July 12 - 14 2010, Munich, Germany.

[9] Quaschning V. (2003), "Technology fundamentals - The sun as an energy resource". Renewable Energy World 6 (5): 90–93.

[10] http://en.wikipedia.org/insolation

[11] Coraggio G., Pisanti C., Rizzo G., Senatore A., (2010), A Moving Solar Roof for a Hybrid Solar Vehicle, IFAC Symposium Advances in Automotive Control, July 12 - 14 2010, Munich, Germany.